Short-pulsed laser transport in absorbing and scattering media: time versus frequency-based approaches

Mathieu Francoeur[1] and Daniel R. Rousse[2]
[1]Department of Mechanical Engineering, University of Kentucky, Lexington, KY 40506, USA.

E-mail: mfran0@engr.uky.edu

[2]Department of Mathematics, Computer Sciences, and Engineering, Université du Québec à Rimouski, Lévis, PQ G6V 8R9, Canada.

E-mail: Daniel_Rousse@uqar.qc.ca

Abstract. Optical tomography (OT) is a promising non-intrusive characterization technique of absorbing and scattering media that uses transmitted and/or reflected signals of samples irradiated with visible or near-infrared light. The quality of OT techniques is directly related to the accuracy of their forward models due to the use of inversion algorithms. In this paper, forward models for transient OT approaches are investigated. The system under study involves a one-dimensional absorbing and scattering medium illuminated by a short laser pulse; this problem is solved using a discrete ordinates – finite volume (DO-FV) method in both the time and frequency-domain. Previous works have shown that time-domain approaches coupled with first order spatial interpolation schemes cannot represent the physics of the problem adequately as transmitted fluxes emerge before the minimal physical time required to leave the medium. In this work, the Van Leer and Superbee flux limiters, combined with the second order Lax-Wendroff scheme, are used in an attempt to prevent this. Results show that despite significant improvement, flux limiters fail to completely eliminate the physically unrealistic behavior. On the other hand, results for transmittance obtained from the frequency-based method are accurate, without physically unrealistic behaviors at early time periods. The frequency-dependent approach is however computationally expensive, since it requires approximately five times more computational time than its temporal counterpart when used as a forward model for transient OT. On the other hand, the great advantages of the frequency-based approach is that limited windows of temporal signals can be calculated efficiently (in transient OT), and it can also be used as forward model for steady-state, frequency-based, and transient OT techniques.

1. Introduction

Optical tomography (OT) techniques refer to the use of low-energy (typically from 10 to 100 mW) radiation, in the visible or near-infrared spectrum, for characterization of absorbing and scattering media. A fraction of the incident light penetrates the absorbing-scattering medium, and is afterwards partially absorbed and scattered into it. The emerging radiation at the boundaries (i.e., transmitted and reflected fluxes) are then measured, and used to infer the radiative properties (absorption and scattering coefficients) of the medium [1]. OT finds applications in many fields, especially in biomedical imaging where non-intrusive tools are needed at low costs and without side effects [1-8].

OT techniques can be divided in three categories: steady-state OT, frequency-based OT, and transient OT. In the first case, a continuous radiation beam is incident upon the medium to be characterized. Steady-state measurements of intensities are done at one of the boundaries of the medium. Biomedical works have reported that steady-state reconstruction algorithms suffer from considerable cross-talk between absorption and scattering coefficients [9,10]; this means that purely scattering (or absorbing) inclusions are reconstructed with unphysical absorption (or scattering) properties [11]. This cross-talk is caused by the fact that different distributions of radiative properties inside the medium can lead to the same value collected at the boundaries [11]. In other words, OT is an ill-posed problem since it has no unique solution.

A way to avoid the so-called cross-talk between the radiative properties is to illuminate the sample with a beam modulated in amplitude (typically at 100-1000 MHz [10,11]). A major advantage of this technique, unlike steady-state OT, is that additional information is obtained by measuring both the amplitude (A) and the phase shift (φ) after multiple scattering and partial absorption in the irradiated sample. Frequency-domain devices then allow a better separation of absorption and scattering coefficients than its steady-state counterpart.

The third alternative is the transient OT technique, which is the object of study of this paper. In this approach, the sample to be characterized is illuminated by a short pulse laser, and the temporal broadening of the pulse, after multiple scattering and partial absorption, is analyzed. The collection of several temporal data per measurement then provides sufficient information to avoid the cross-talk between the radiative properties of the sample.

The estimation of the radiative properties of an irradiated medium from its transmitted/reflected signal is possible via an inversion algorithm. Many inverse techniques for the three types of OT have been developed, and are all based on minimization procedures (see for example [9,11-15]). This implies that the quality of the inversion, and consequently the characterization, is directly related to the accuracy of the forward model.

Short-pulsed laser transport in absorbing and scattering media can be accurately modeled by the transient radiative transfer equation (TRTE). The distinction between the standard steady-state radiative transfer equation (RTE) and TRTE is made here since transient effects associated with radiation transfer can be neglected when the time needed by the photons to leave a medium is shorter than the period of variation of the radiative source, which is the case in most engineering applications. In transient OT, the pulse laser is generally of the order of picosecond to femtosecond, which involves non-negligible transient effects.

A wide variety of computational methods have been developed in order to solve the TRTE, which describes the spatial and temporal variations of the radiation intensity into a participating medium along a particular direction. Among these methods: the traditional [16,17] and reverse [18] Monte Carlo formulations, the classical spherical harmonics [19], the modified $MP_{1/3}A$ [20], the two-flux approaches [19], the radiation element methods [21], the discrete ordinates approaches [22-24], the integral formulations [25,26], the backward method of characteristics [27,28], the discrete transfer method [29], and the Galerkin approach [30,31].

In this paper, a discrete ordinates - finite volume (DO-FV) method is proposed to solve a one-dimensional problem in Cartesian coordinates. The reasons underlying this choice can be summarized as follows: (1) it makes use of an appropriate representation of the angular dependence of the radiation intensity, (2) it allows simplicity of implementation and solution, and can be extended easily to multidimensional geometries, and (3) it involves relatively short computational times for convergence.

Direct solution of the TRTE with a DO-FV approach causes some problems. Indeed, it is quite well known that time-based DO-FV approaches induces transmitted radiative fluxes that emerge earlier than the minimal time required by the radiation to leave the medium [22-24,32]. This is caused mainly by the interdependence between the spatial and temporal discretizations, and the numerical approximations embedded within the application of an interpolation scheme. Here, these unphysical results associated with the propagation of a sharp wave front are minimized by the implementation of a second order interpolation scheme (Lax-Wendroff) coupled with flux limiters into the DO-FV as some researchers [22-24,33,34] have proposed similar ideas in attempts to overcome the problem.

On the other hand, the interdependence between the spatial and temporal discretizations can be avoided by solving the transient radiative transfer problem in the frequency-domain. This idea, originally proposed by Elaloufi et al. [35] to assess the use of the Diffusion approximation and adapted later by Francoeur et al. [36] to determine the optimal conditions of a frequency-based OT, is to transform the temporal variables into frequency-dependent variables by applying a Fourier transform. This leads to the so-called complex radiative transfer equation (CRTE), which must be solved for each frequency contained in the incident pulse. In this paper, the DO-FV method is also used for the solution of the CRTE. The frequency-based approach for solving transient radiative transfer problems has also been applied recently in conjunction with a discontinuous finite element method [37].

The main objective of this paper is to compare the time and frequency-based approach when applied to solve problems involving short-pulsed laser propagation in absorbing and scattering media (i.e., forward model of the transient OT). The theoretical formulation is summarized in the second section: the problem is described, the assumptions are formulated, and the mathematical models are presented. The DO-FV formulations, both in the time and frequency-domain, are afterwards the subject matter of section 3. The methods are then applied to two typical one-dimensional transient radiative transfer problems, and results are compared with those obtained with a first order exponential scheme [32] and with those available in the literature. Concluding remarks are presented in the fifth section of the paper.

2. Theoretical formulation

2.1. Description of the problem and assumptions

Throughout this paper, the following assumptions apply: (1) the medium is a plane-parallel semi-infinite layer of thickness z_L; (2) the layer is composed of an non-emitting, absorbing and scattering homogeneous medium, with a relative refractive index of unity; (3) radiative properties are calculated at the central wavelength of the pulse's spectral bandwidth and, consequently, reference to wavelength is omitted in the notations; (4) scattering is assumed to be independent; (5) boundaries are transparent; (6) the layer is subject to a collimated short square pulse of radiation at normal incidence (the problem is azimuthally symmetric); (7) a pure transient radiative transfer regime is considered, i.e. the pulse width is less than the characteristic time for the establishment of any other phenomenon [19]. This one-dimensional transient radiative transfer problem is schematically depicted in figure 1.

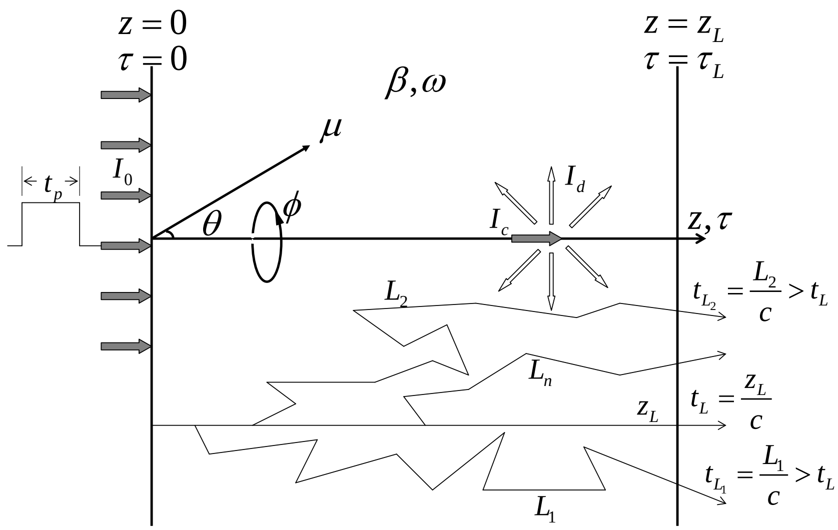

Figure 1. Schematic representation of a transient radiative transfer problem.

The fraction of the incident collimated radiation beam which is not scattered crosses the medium in a straight line. Therefore, for this fraction of the beam, the time required to leave the medium is the shortest that is $t_L = z_L/c$. For an optically thick and highly scattering medium, an important part of the photons are scattered in all directions (travel paths L_1 and L_2). Therefore, the time required by these photons to leave the medium at the boundary $z = z_L$ is necessarily greater than t_L, since the traveling distances are longer. This means that the total duration of the transmitted radiative flux at the boundary $z = z_L$ (called the transmittance) is longer than the duration of the pulse. This transmitted signal is dependent on the radiative properties of the medium, since its duration and shape are dependent of the traveling paths of the photons inside the medium. In turn, the traveling paths are directly related to the absorption and scattering coefficients. The analysis of temporal distributions and broadening of transmitted fluxes constitutes the basis of transient OT techniques. A similar conclusion holds with respect to temporal distributions of the reflectance. It is also important to point out that only limited windows of temporal transmitted/reflected signals might be needed for OT purpose. Indeed, it has been shown that the transmitted peak of radiation is mostly related to the scattering response of the irradiated medium, while its trailing part is mostly due to absorption [38]. Therefore, a sensitivity analysis on the temporal signals obtained from the forward model would help to determine the optimal temporal zones for the estimation of a given parameter.

2.2. Mathematical modeling

Since the problem deals with collimated irradiation, the most convenient approach to fulfill this need for a mathematical solution is to consider a separate treatment of the diffuse-scattered component (I_d) of the radiative intensity [39]. Variations of the collimated intensity (I_c) are simply described by a spatial exponential decay and a temporal term originating from the propagation of the pulse [22]. On the other hand, the TRTE describes spatial and temporal variations of the diffuse component of the intensity along a direction μ in the absorbing and scattering medium. Using dimensionless time ($t^* = \beta c t$) and optical depth ($\tau = \beta z$) as variables, the TRTE in one-dimensional Cartesian coordinates is written as follows [39]:

$$\frac{\partial I_d(\tau,\mu,t^*)}{\partial t^*} + \mu \frac{\partial I_d(\tau,\mu,t^*)}{\partial \tau} = -I_d(\tau,\mu,t^*) + \frac{\omega}{2}\int_{-1}^{1} I_d(\tau,\mu',t^*)\Phi(\mu',\mu)d\mu' + S_c(\tau,\mu,t^*) \quad (1)$$

where β and ω are the attenuation coefficient (out-scattering and absorption) and albedo for single scattering, respectively. The first and second terms on the right-hand side of equation (1) represent respectively the total attenuation, and the reinforcement due to the scattering of the diffuse part of intensity (i.e., in-scattering). In the particular case of a square pulse of dimensionless duration t_p^*, the radiation source term S_c, due to the scattering of the collimated intensity, is given by [22]:

$$S_c(\tau,\mu,t^*) = \frac{\omega}{4\pi} I_0 \exp(-\tau)[H(t^* - \tau) - H(t^* - t_p^* - \tau)]\Phi(1,\mu) \qquad (2)$$

where the variable $\Phi(1,\mu)$ implies that the collimated radiation beam is in normal incidence. Equations (1) and (2) constitute the mathematical model when the problem in solved in the space-time domain.

Alternatively, when the problem is solved in the space-frequency domain, all temporal variables have to be transformed into frequency-dependent variables by applying a temporal Fourier transform (FT) of the intensity [35]:

$$I(\tau,\mu,t^*) = \int_{-\infty}^{\infty} \hat{I}(\tau,\mu,\hat{\omega}) \exp(i\hat{\omega}t^*) d\hat{\omega} \qquad (3)$$

where $\hat{\omega}$ is the angular frequency derived from the dimensionless time variable t^*. Inversely, the frequency-dependent intensity can be written as the FT of the time-dependent intensity. The time-dependent Fourier analysis applied to the TRTE (equation (1)) leads to:

$$\mu \frac{d\hat{I}_d(\tau,\mu,\hat{\omega})}{d\tau} = -(1+i\hat{\omega})\hat{I}_d(\tau,\mu,\hat{\omega}) + \frac{\omega}{2}\int_{-1}^{1} \hat{I}_d(\tau,\mu',\hat{\omega})\Phi(\mu',\mu)d\mu' + \hat{S}_c(\tau,\mu,\hat{\omega}) \,. \qquad (4)$$

where the frequency-dependent intensity $\hat{I}_d(\tau,\mu,\hat{\omega})$ and $(1+i\hat{\omega})$ are complex numbers. This equation has the form of a steady-state radiative transfer equation and is called the complex radiative transfer equation (CRTE) [36]. The source term $\hat{S}_c$ originating from the scattering of the collimated intensity is determined from a particular solution of equation (4) without scattering sources [35]:

$$\hat{S}_c(\tau,\mu,\hat{\omega}) = \frac{\omega}{4\pi} \hat{I}_0(\hat{\omega}) \exp[-\tau(1+i\hat{\omega})]\Phi(1,\mu) \,. \qquad (5)$$

Equations (4) and (5) constitute the mathematical model when the problem is solved in the frequency-domain. The variable $\hat{I}_0(\hat{\omega})$ in equation (5) is obtained from the temporal Fourier analysis of the incident pulse; this is schematically depicted in figure 2.

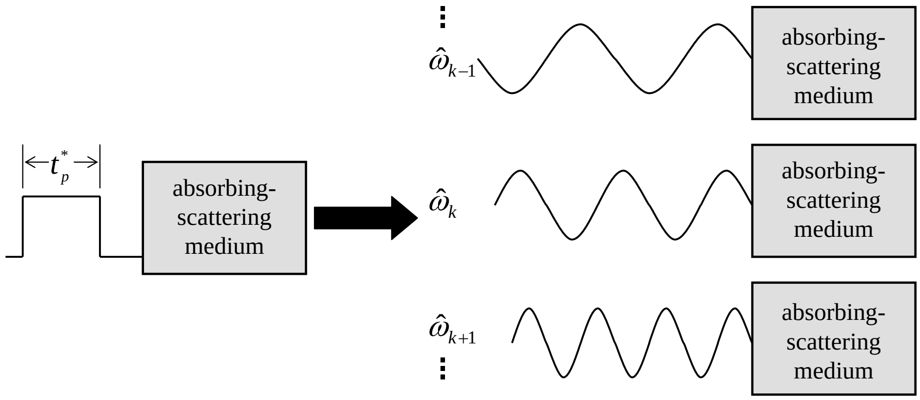

Figure 2. Shift from the space-time to the space-frequency domain.

From the above statement and figure 2, it is concluded that the solution of a transient radiative transfer problem can be obtained by solving the CRTE for each angular frequency contained in the temporal Fourier decomposition of the pulse.

3. Numerical solution

For both time and frequency-based approaches, a discrete ordinates – finite volume (DO-FV) method is adopted. The DO approach is used for the angular discretization, while FV refers to the spatial discretization.

3.1. Time-based DO-FV formulation

The radiation intensity, following the assumptions stated in the previous section, is space, direction, and time-dependent. It is therefore necessary to discretize these three independent variables in order to solve the TRTE numerically.

The spatial domain is discretized in J non-overlapping control volumes $\Delta\tau_j$. The method implemented here also involves a discretized angular domain into M directions of equal angular weight w_m [39]. This uniform angular discretization respects the half-range first moment as well as the full-range zeroth moment to fulfill this need for energy conservation [40]. Finally, the temporal variations of the TRTE are approximated by defining N finite time steps Δt_n^*. Then, integrating the TRTE over a control space $\Delta\tau_j w_m \Delta t_n^*$ with a temporal implicit scheme yields:

$$I_j^{m,n} = \frac{\dfrac{1}{\Delta t_n^*} I_j^{m,n-1} - \dfrac{\mu_m}{\Delta\tau_j}\left(I_{j+1/2}^{m,n} - I_{j-1/2}^{m,n}\right) + \dfrac{\omega_j}{2}\sum_{m'=1}^{M} w_{m'} I_j^{m',n} \Phi_j^{m'm} + S_{c_j}^{m,n}}{\dfrac{1}{\Delta t_n^*} + 1} \tag{6}$$

In the above, $I_j^{m,n}$ is the intensity at node j, in direction m, and at time step n, while $I_{j\pm 1/2}^{m,n}$ are the intensities at the boundaries of the control volume. The subscript d, referring to the diffuse component of the intensity, is omitted for clarity.

To solve equation (6), one needs to relate the value of the intensity at a node (…, j – 1, j, j + 1,…) – for a specific direction and time step – to the value of the intensity at control volume faces (j ± ½). When an appropriate spatial interpolation scheme is selected, equation (6) is then solved for each node j, in each direction m, and for each time step n of the spatial, angular, and temporal discretizations, respectively. An iterative scheme, based upon the convergence of the source term due to the scattering of the diffuse part of intensity, is used.

In steady-state radiative heat transfer problems, first order interpolation methods, such as the upwind scheme, are usually sufficient. In transient radiative transfer, the situation is different since the problem involves the propagation of a sharp front (i.e., the pulse). The moving pulsed collimated radiation beam in an absorbing and scattering medium is schematically depicted in figure 3. This figure can be seen as a snapshot of the wave front of the pulse at a particular instant t_n^*.

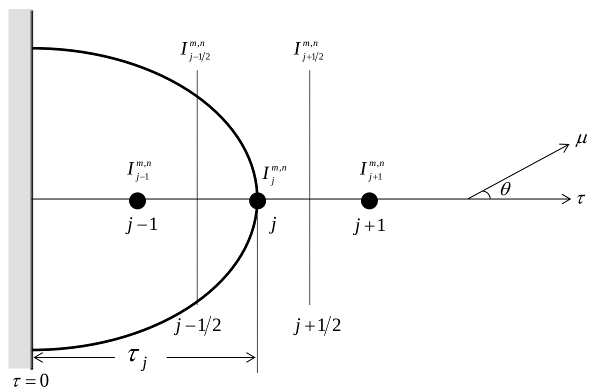

Figure 3. Schematic representation of a pulsed collimated radiation beam propagating in a participating medium.

As described in figure 3 at instant t_n^*, the front of the pulse is located at position τ_j (node j). Consequently, from a theoretical point of view, intensities located within the range of the front of the pulse ($\tau \leq \tau_j$) are necessarily greater than zero, while intensities located beyond this front ($\tau > \tau_j$) are equal to zero. However, from a numerical point of view, intensities at nodes j + 1, j + 2, …, J could be non-zero due to the numerical approximations embedded in any interpolation schemes. This temporal numerical diffusion then lead to radiative fluxes emerging earlier than the minimal time required by the radiation to leave the medium [32]. These early transmitted radiative fluxes can be partially minimized by applying the Courant stability criteria expressed here as: $\Delta t_n^* < \min\{\Delta\tau_j\}$ [32,41]. This condition simply ensures that for a given temporal step, the wave front of the pulse can not propagate within more than one control volume at a time. Here, the Courant number C_0 has been defined as $\Delta t_n^*/\min\{\Delta\tau_j\}$.

However, the application of the Courant stability criteria and a first order interpolation scheme has been found to be insufficient and the second order spatial interpolation Lax-Wendroff (L-W) scheme, originally proposed for Eulerian transport problems in hydrodynamics, is used in this work [41]. This scheme, based on the decomposition of the dependent variable (radiation intensity) into Taylor series expansion truncated after the second order term, implies (for $\mu > 0$) [41]:

$$I_{j+1/2}^{m,n} = I_j^{m,n} + \frac{1}{2}(1 - \Delta t_n^* / \Delta\tau_j)(I_j^{m,n} - I_{j-1}^{m,n}) \tag{7}$$

Equation (7) stipulates that the intensity at the boundary j + 1/2 of the control volume is computed with a linear interpolation (figure 4), where the slopes are represented by Δ_+ (between nodes j and j +1) and Δ_- (between nodes j – 1 and j).

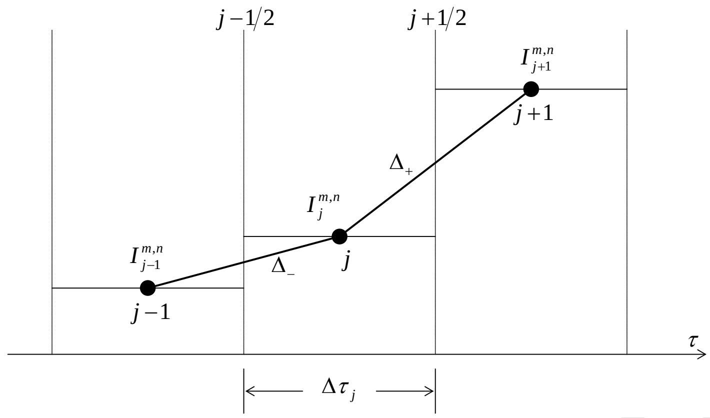

Figure 4. Representation of a control volume and its surrounding nodes.

This numerical approach has been found to reduce the temporal numerical diffusion, but introduces, in counterpart, significant oscillations near the discontinuity (i.e., at the front of the pulse) [41]. In that case, a correction factor must be introduced in order to ensure a monotonicity preserving scheme [22,34,42]. Such a monotonicity preserving scheme ensures that when the initial distribution of a moving quantity is monotonic, the resulting distribution is also monotonic. In other words, this condition prevents the creation of false extremas, or a false amplification of existing extremas (i.e., eliminates the oscillations).

The introduction of a flux limiter Ψ_j in equation (7) enables one to keep the solution monotonic and allows the accuracy of a second order spatial interpolation scheme. The L-W scheme is consequently modified such that (for $\mu > 0$) [34,41]:

$$I_{j+1/2}^{m,n} = I_j^{m,n} + \frac{1}{2}\Psi_j(1-\Delta t_n^*/\Delta\tau_j)(I_j^{m,n} - I_{j-1}^{m,n}) \tag{8}$$

The value of Ψ_j must be determined by the spatial distribution of intensity; this is done by the introduction of the variable r_j [34]:

$$r_j = \frac{I_{j+1}^{m,n} - I_j^{m,n}}{I_j^{m,n} - I_{j-1}^{m,n}} \tag{9}$$

The right-hand side of equation (9) simply represents the ratio of the slopes Δ_+ and Δ_- in the particular case of a regular spatial discretization (see figure 4). In this work, the Van Leer flux limiter is used, and is written as [34,41]:

$$\Psi_j = \frac{r_j + |r_j|}{1+|r_j|} \tag{10}$$

Equation (10) implies that when there is a discontinuity around node j (slopes Δ_+ and Δ_- of opposite signs), r_j takes a negative value and the flux limiter Ψ_j becomes equal to zero. Consequently, equation (8) reduces to the first order upwind scheme. On the other hand (slopes Δ_+ and Δ_- of same signs), the interpolation slope at the node j is determined by the harmonic mean of the slopes Δ_+ and Δ_-. Another flux limiter, called Superbee, is used in this paper, and is defined as [34,41]:

$$\Psi_j = \max[0, \min(1, 2r_j), \min(r_j, 2)]. \tag{11}$$

In this case, the value of Ψ_j is determined by comparing the slopes Δ_+ and Δ_- around node j. As for the Van Leer flux limiter, Ψ_j equals zero when the slopes Δ_+ and Δ_- are of opposite signs. It is important to note that numerical details regarding flux limiters are beyond the scope of this paper, and are available elsewhere [41].

3.2. Frequency-based DO-FV formulation

The same type of numerical approach is used to solve the CRTE. For a given angular frequency $\hat{\omega}$, a steady-state radiation transport problem is solved by calculating the frequency-dependent intensities on the J nodes and M directions of the spatial and directional discretizations, respectively. Then, integrating the CRTE over a control space $\Delta\tau_j w_m$ yields:

$$\hat{I}_j^{m,k} = \frac{\dfrac{-\mu_m}{\Delta\tau_j}\left(\hat{I}_{j+1/2}^{m,k} - \hat{I}_{j-1/2}^{m,k}\right) + \dfrac{\omega_j}{2}\sum_{m'=1}^{M} w_{m'} \hat{I}_j^{m',k} \Phi_j^{m'm} + \hat{S}_{c_j}^{m,k}}{1 + i\hat{\omega}_k}. \tag{12}$$

In the above, $\hat{I}_j^{m,k}$ is the frequency-dependent intensity at node j, in direction m, and at frequency k, corresponding to the discrete pulsation $\hat{\omega}_k$ for which the CRTE is solved. The subscript d, referring to the diffuse component of intensity, is omitted for more clarity. The spatial and directional solutions of the CRTE are exactly the same than for the TRTE. For the frequency-dependent approach, a first order upwind scheme is sufficient for proper interpolation, since the CRTE is a steady-state equation; the numerical implementation is thus greatly simplified.

In order to determine the frequencies for which the CRTE is solved, a temporal FT is applied on the incident square pulse:

$$I_0^k = I_0\left(\frac{\sin\hat{\omega}_k t_p^*}{\hat{\omega}_k} - i\frac{1-\cos\hat{\omega}_k t_p^*}{\hat{\omega}_k}\right). \tag{13}$$

The K relevant angular frequencies are selected by calculating equation (13) for a series of discrete pulsations $\hat{\omega}_k$. A graphical representation of the real and imaginary parts of I_0^k, as a function of $\hat{\omega}_k$, allows one to find the threshold angular frequencies, $\hat{\omega}_{-K/2}$ and $\hat{\omega}_{K/2}$, for which the CRTE has to be solved (i.e., frequencies below and above which the real and imaginary parts of I_0^k vanish). The angular frequency discretization $\Delta\hat{\omega}_k$ is determined, as for the spatial discretization, by performing a numerical sensitivity analysis [36].

Finally, the time-dependent intensities have to be recovered from the frequency-dependent intensities. This is done by applying an inverse Fourier transform (IFT) on the frequency-dependent intensities:

$$I_j^{m,n} = \mathrm{Re}\left\{2\sum_{k=0}^{K/2}\frac{1}{K}\exp(i\hat{\omega}_k t_n^*)\hat{I}_j^{m,k}\right\}. \tag{14}$$

Equation (14) implies that the frequency-dependent intensities can be calculated and summed only for the $K/2$ relevant angular frequencies (symmetry of the summation) in order to determine the time-dependent intensity at a given instant t_n^*. Unlike the space-time approach, the determination of the intensity at instant t_n^* doesn't require the knowledge of intensities at 0, t_1^*, t_2^*, …, t_{n-1}^*.

The principal steps to solve the transient radiative transfer problem in the space-frequency domain are summarized hereafter: (1) the temporal FT of the pulse is calculated; (2) the relevant frequencies are determined; (3) a CRTE is solved for each selected angular frequency; (4) an IFT is applied in order to derive time-dependent intensities.

4. Results and discussion

Two transient radiative transfer problems are solved in this section; in both cases, the absorbing and scattering medium is illuminated by a square pulsed collimated radiation beam of unit intensity (I_0 = 1) and unit dimensionless duration (t_p^* = 1) on its boundary at $\tau = 0$ (see figure 1). When the medium is anisotropically scattering, the linear anisotropic phase function is considered ($\Phi(\mu,\mu') = 1 + a\mu\mu'$) [39].

In post-treatment, the temporal hemispherical transmittance is calculated from the time-dependent intensities, and is given by:

$$T^n = \frac{2\pi \sum_{\mu_m > 0} w_m \mu_m I_J^{m,n} + I_{c_J}^{m_0,n}}{I_0}. \qquad (15)$$

The codes have been written in *FORTRAN* and compiled with *Microsoft Developer Studio – Fortran PowerStation 4* on a single processor desktop PC.

4.1. Problem 1: Optically thick and highly scattering medium

In this first problem, the optical thickness of the medium is τ_L = 10 while the scattering albedo is ω = 0.998, values that are typical for biological tissues. The transmittance is calculated for three types of scattering media: isotropic (a = 0), highly forward scattering (a = 0.9), and highly backward scattering (a = -0.9). For this problem, 100 spatial nodes and 10 directions are sufficient to discretize the spatial and directional domains; no significant improvement of the results has been observed beyond these thresholds. The temporal discretization is determined by analyzing the Courant number; numerical simulations have been performed, and a Courant number of 0.2 has been found to be optimal (results not presented).

Transmittances obtained from the DO-FV and the Van Leer flux limiters are presented in figure 5, and compared with those obtained from a Monte Carlo (MC) formulation [17]. It is important to note that since the optical thickness of the slab is 10, the minimal dimensionless time required by the radiation to leave the medium is also 10.

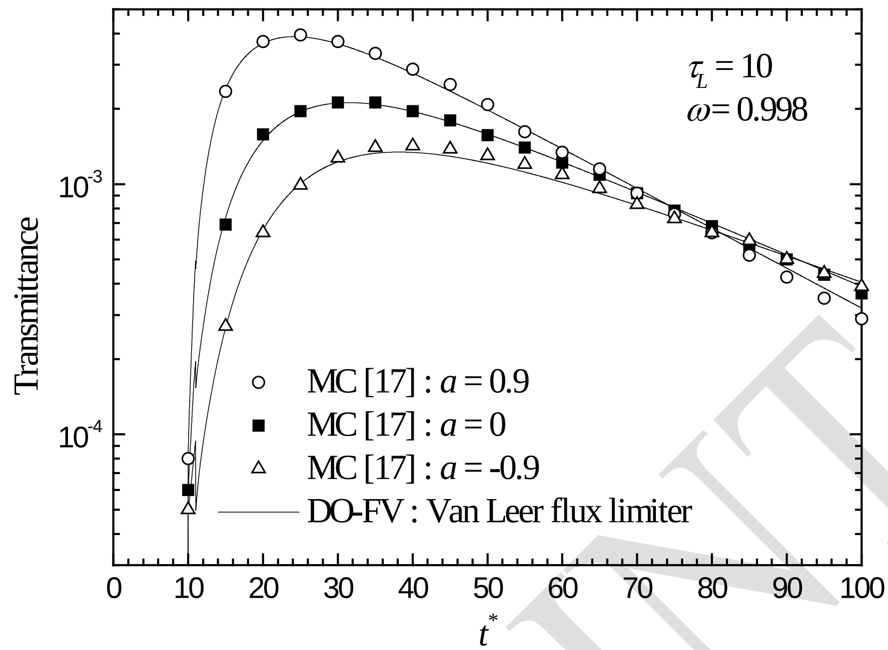

Figure 5. Temporal distribution of the hemispherical transmittance; comparison between the Van Leer flux limiter and a Monte Carlo formulation [17].

The sharp diminution of transmittance at t^* = 11, followed by an increase (more visible for the case a = -0.9), is due to fact that the collimated component of intensity has left the medium (square pulse of dimensionless duration t_p^* = 1). A highly forward scattering medium (a = 0.9) leads to a higher maximum of transmittance, since this phase function tends to throw the scattered photons at the boundary $\tau = \tau_L$. On the other hand, a highly backward scattering phase function (a = -0.9) produces longer travel paths of the scattered photons, leading to a weaker maximum of transmittance. For a longer period of time, the transmittance is higher for the backward scattering phase function (from $t^* \approx$ 85) due to a more important photons retention.

Figure 5 clearly indicates that for a large time scale (from 0 to 100), results obtained with the Van Leer flux limiter are in good agreement with those obtained with a reference Monte Carlo approach, even at early time periods. The same conclusion is applicable for the Superbee flux limiter (results not shown)

When the problem is solved in the frequency domain, the temporal Fourier transform of the square pulse allows the determination of pulsations for which the CRTE has to be solved (from -16π to 16π, except $\hat{\omega}_k$ = 0). A preliminary parametric analysis permitted the identification of an optimal angular frequency discretization ($\Delta\hat{\omega}_k = 3\times 10^{-4}\pi$). Transmittances obtained by solving the CRTE and a first order upwind scheme are reported in figure 6.

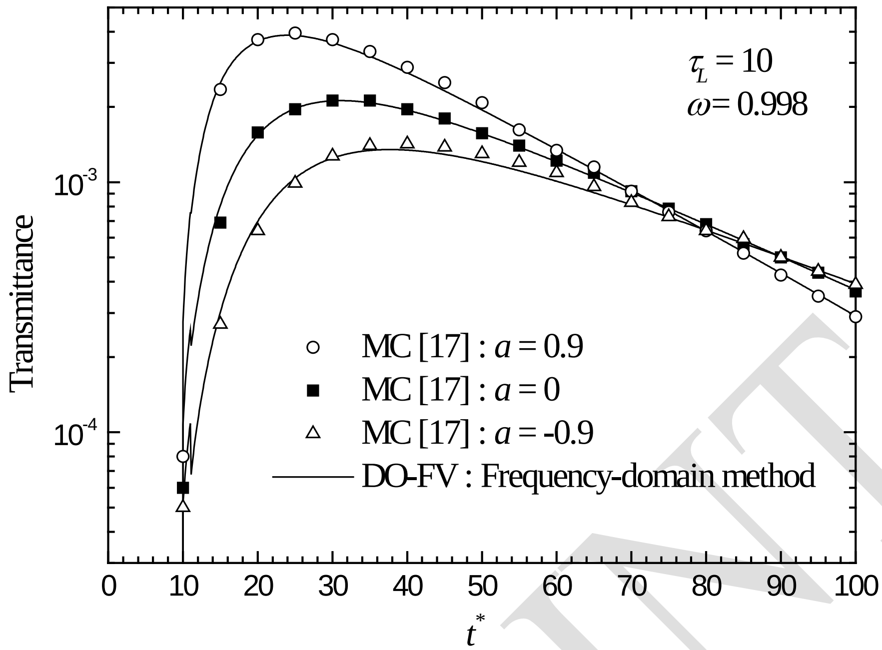

Figure 6. Temporal distribution of the hemispherical transmittance; comparison between the frequency-domain approach and a Monte Carlo formulation [17].

Similar than for the space-time approach, figure 6 indicates that for a large time scale (from 0 to 100), results are in good agreement with those obtained from a MC formulation [17].

In order to analyze more precisely the relative accuracy of the different approaches, the transmittances obtained from the frequency-domain method are compared at early time periods, in figure 7, with those obtained with a first order exponential scheme [32], the Van Leer flux limiter and the Superbee flux limiter. Only results for a = 0.9 are shown, since early transmitted radiation becomes more important within a highly forward scattering medium.

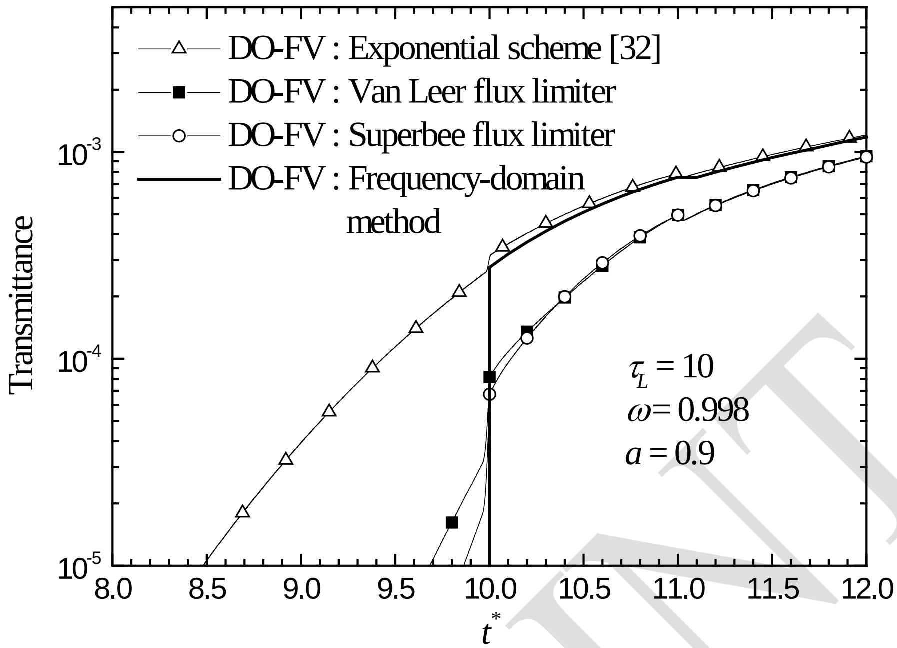

Figure 7. Temporal distribution of hemispherical transmittance; comparison between the Van Leer flux limiter, the Superbee flux limiter, the exponential interpolation scheme [32], and the frequency-domain method at early time periods.

Figure 7 shows that the radiative flux leaving the medium before the minimal physical dimensionless travel time t_L^* = 10 is considerably decreased with the flux limiters. Generally, for all simulations carried out, the Superbee flux limiter lead to more accurate results than the Van Leer. Despite this fact, early transmitted radiation can not be completely avoided. On the other hand, no energy is transmitted before t_L^* = 10 with the frequency-dependent method, since there is no interdependence between the spatial and temporal discretizations.

It can be concluded that, from a strict point of view of accuracy, the frequency-dependent method is superior than solving directly the TRTE in the space-time domain, since the transmittance begins exactly at the dimensionless time t^* = 10. Even after this instant, the approaches give different results, and converged to the same values approximately between t^* = 10 and $t^* \approx 12$. However, the temporal resolution of the available MC results [17] is insufficient to conclude about this divergence.

The CPU times associated with the different methods are presented in table 1, and have been compiled for the case of an isotropic scattering medium (a = 0).

Table 1. CPU times associated with different time-based approaches and the frequency-based method for problem 1.

Method	CPU time [s]	Relative CPU time (Superbee flux limiter) [-]
Time-domain approach, exponential scheme	156	0.60
Time-domain approach, Van Leer flux limiter	238	0.91
Time-domain approach, Superbee flux limiter	262	1

Frequency-domain approach	1343	5.13

The frequency-dependent approach is time consuming: a large number of frequencies is required to model a square pulse, and the shift from the space-frequency to the space-time domain (IFT) constitutes a supplementary computational step, compared to the direct solution of the TRTE. For this particular problem, the frequency-dependent method requires approximately five times more CPU time than solving the problem in the space-time domain with a Superbee flux limiter.

4.2. Problem 2: Medium of unit optical thickness and variable scattering albedo

In this second problem, the optical thickness of the medium is fixed at $\tau_L = 1$ while the scattering albedo ω is variable (0.25, 0.50, 0.75 and 0.90). In all cases, the medium is isotropically scattering (a = 0). This second test problem has been solved with a discrete ordinates approach coupled with the piecewise parabolic advection scheme (DO-PPA) [22], which has been validated with a Monte Carlo formulation [17]. The same spatial, angular, and temporal discretizations used for the first problem are found sufficient.

The transmittances, obtained from the DO-FV method coupled with the Van Leer (not shown) and Superbee flux limiters (figure 8) have been calculated. In this case, the minimal dimensionless time needed by the radiation to leave the slab of unit optical thickness is $t_L^* = 1$.

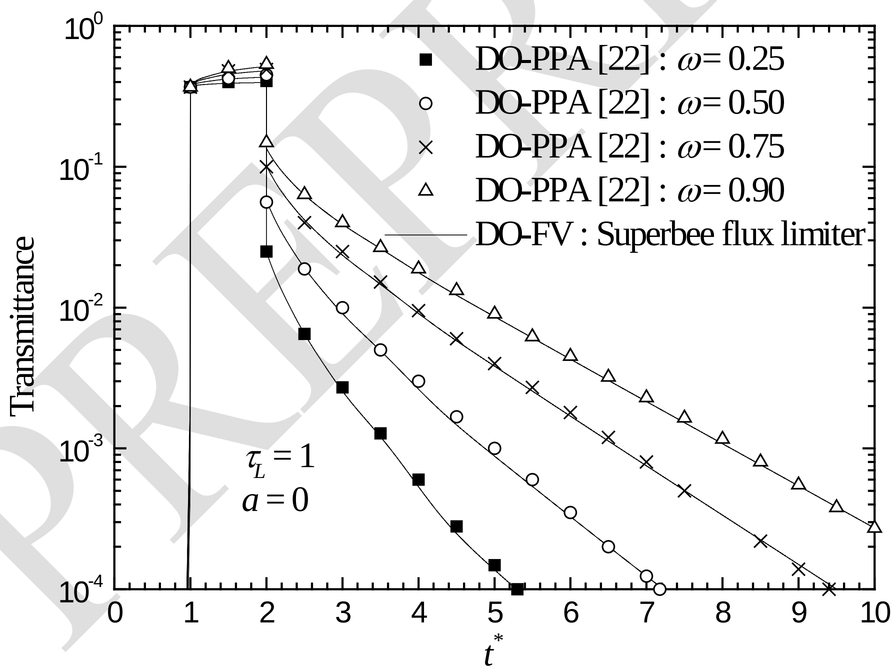

Figure 8. Temporal distribution of the hemispherical transmittance; comparison between the Superbee flux limiter and the DO-PPA method [22].

The transmittance is more important as the scattering albedo increases. This can be explained by the fact that a larger proportion of the pulsed collimated radiation beam is scattered in the medium. Moreover, an increase of the scattering albedo leads to a diminution of the mean free path of scattering, and hence to an increase of multiple scattering, longer photons travel paths, and, consequently, a larger transmitted temporal signal. Here again, the decrease of transmittance at $t^* = 2$ is due to the fact that the collimated component of radiation intensity has left the medium. After $t^* = 2$, the transmittance is only due to the diffuse part of radiation intensity.

It can be seen in figure 8 that the temporal distributions of transmittances are, in general, in good agreement with those obtained from the DO-PPA. However, early transmitted radiation can be observed on a temporal scale from 0 to 10; the same conclusions hold for the Van Leer flux limiter.

Transmittances from the frequency-dependent approach are presented in figure 9.

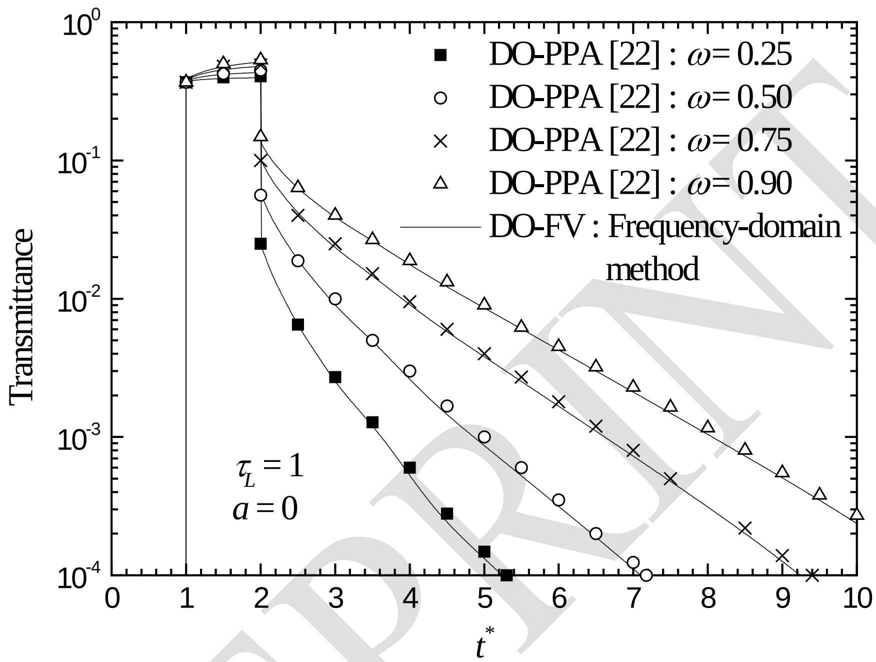

Figure 9. Temporal distribution of hemispherical transmittance; comparison between the frequency-domain approach and the DO-PPA method [22].

As for the first problem, results from the space-frequency method are in good agreement with those from the literature [22]. It can also be seen that the physics of the problem is respected, since the transmittance begins exactly at $t^* = 1$.

A comparison between the frequency and time-dependent methods (exponential scheme [32], Van Leer flux limiter, and Superbee flux limiter), at early time periods, is shown in figure 10.

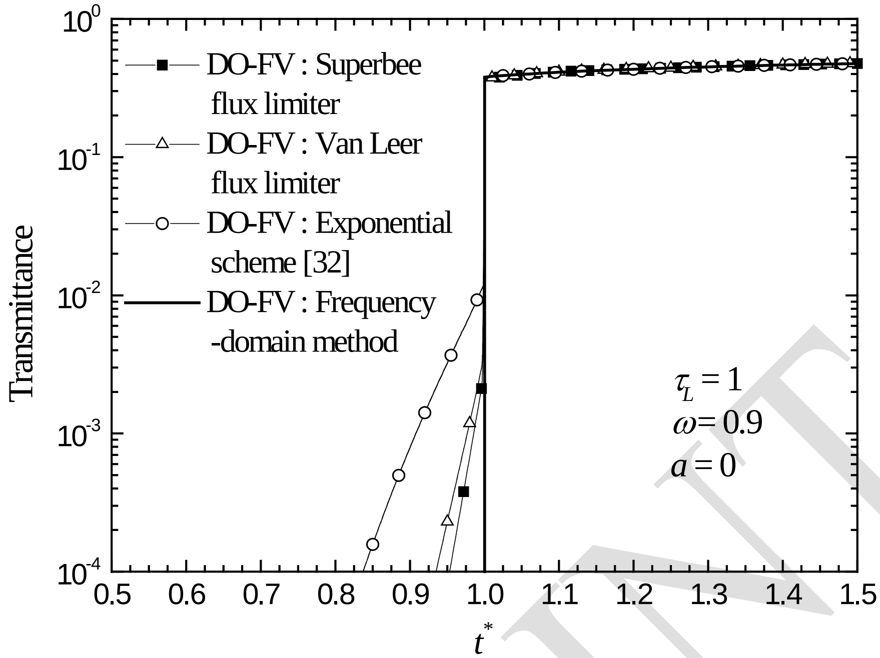

Figure 10. Temporal distribution of hemispherical transmittance; comparison between the Van Leer flux limiter, the Superbee flux limiter, the exponential interpolation scheme [32], and the frequency-domain method at early time periods.

Again, early transmitted radiation fluxes are completely avoided with the frequency-domain method. Also, inversely to what has been observed for the first problem (figure 7), figure 10 does not report significant differences between the two approaches after t_L^*. This can be explain by the fact that, for a medium of unit optical thickness, the ballistic regime (collimated component) is dominant compared to the sinuous propagation regime (diffuse component), in the beginning of the temporal process. Hence, the collimated intensity does not induced early transmitted radiation, since its solution is determined exactly by a spatial exponential decay.

The CPU times associated with the different solution approaches are presented in table 2, when the scattering albedo is 0.9; the conclusions stated for problem 1 are again applicable here.

Table 2. CPU times associated with different time-based approaches and the frequency-based method for problem 2.

Methods	CPU time [s]	Relative CPU time (Superbee flux limiter) [-]
Time-domain approach, exponential scheme	143	0.57
Time-domain approach, Van Leer flux limiter	225	0.89
Time-domain approach, Superbee flux limiter	252	1
Frequency-domain approach	1303	5.17

5. Conclusion

One-dimensional transient radiative transfer problems for absorbing and scattering media have been solved in Cartesian coordinates using a discrete ordinates – finite volume (DO-FV) approach, in both the time and frequency-domain. The Van Leer and Superbee flux limiters, based on the second order spatial scheme Lax-Wendroff, have been used in order to minimize the transmitted fluxes emerging before the minimal time required by the radiation to leave the medium when the problem is solved in the time-domain. In general, results from the DO-FV coupled with flux limiters are in close agreement with those from the literature. Moreover, a comparison at early time periods with the transmittance obtained from a DO-FV and a first order exponential scheme has shown that the flux limiters can substantially decrease the temporal numerical diffusion. However, there is still a low transmitted flux before the minimal physical time required by the radiation to leave the medium.

It has been also shown that temporal distributions of transmittance obtained from the frequency-domain approach are accurate, without physically unrealistic behavior at early time periods. However, compared to a time-dependent approach, the space-frequency method is time consuming (requires approximately five times more CPU time than solving directly the TRTE with a Superbee flux limiter). A fast Fourier transform (FFT) algorithm was implemented to accelerate the inverse Fourier transform (IFT) step, but the success of this strategy was mitigated: no significant improvement in CPU time was reported (unpublished). The reason is that the IFT itself is not what burdens the algorithms, and the large CPU time are mostly due to the large numbers of angular frequencies needed to correctly represent the square pulse. Therefore, a more physically realistic Gaussian incident pulse must be taken into account, since less angular frequencies will be required to adequately represent this temporal pulse.

The motivations underlying these research works are to provide accurate forward models to be used in inverse procedure for optical tomography (OT) applications. Here, the relative accuracy and efficiency of forward models for transient OT have been investigated. One of the advantage of solving the CRTE, instead of the TRTE, is that it can be applied to all kinds of OT techniques (steady-state, frequency-based, and transient), which makes this forward mathematical model highly versatile. Also, as pointed out in the paper, in transient OT, the entire temporal distribution of transmitted/reflected radiation is generally not needed. When the forward model is based on the TRTE, the intensity at time step n requires the solution of the problem at time step $n - 1$, $n - 2$, …, 1. When solving the CRTE, the intensity at instant n can be calculated without prior knowledge of the temporal distribution.

The next step of the project is therefore devoted to the implementation of the frequency-domain approach to multidimensional problems. Sensitivity analyses will also be performed to determine optimal temporal windows of intensities where a given parameter (absorption and scattering coefficients) can be estimated accurately.

Acknowledgments
The authors are grateful to the Natural Sciences and Engineering Research Council of Canada (NSERC) for their financial support.

References

[1] Arridge S R 1999 Optical tomography in medical imaging *Inverse Problems* **15** R41-R93.

[2] Yodh Y and Chance B 1995 Spectroscopy and imaging with diffusing light *Physics Today* **48**(3) 34-40.

[3] Hebden J, Arridge S and Delpy D 1997 Optical imaging in medicine: I. Experimental techniques *Physics in Medicine and Biology* **42** 825-840.

[4] Hielscher A H 2005 Optical tomographic imaging of small animals *Current Opinion in Biotechnology* **16**(1) 79-88.

[5] Scheel A K, Backhaus M, Klose A D, Moa-Anderson B, Netz U, Hermann K G, Beuthan J, Müller G A, Burmester G R and Hielscher A H 2005 First clinical evaluation of sagittal laser optical tomography for detection of synovitis in arthritic finger joints *Annals of the Rheumatic Diseases* **64** 239-245.

[6] Hielscher A H, Klose A, Scheel A, Moa-Anderson B, Backhaus M, Netz U, Beuthan J 2004 Sagittal laser optical tomography for imaging of rheumatoid finger joints *Physics in Medicine and Biology* **49**(7) 1147 - 1163.

[7] Zhu Q, Cronin E B, Currier A A, Vine H S, Huang M, Chen N and Xu C 2005 Benign versus malignant breast masses: optical differentiation with US-guided optical imaging reconstruction *Radiology* **237**(1) 57-66.

[8] Zhang Q and Jiang H 2006 Three-dimensional diffuse optical imaging of hand joints: system description and phantom studies Optics and Lasers in Engineering **43**(11) 1237-1251.

[9] Klose A D and Hielscher A H 2002 Optical tomography using the time-independent equation of radiative transfer-Part 2: inverse model *Journal of Quantitative Spectroscopy and Radiative Transfer* **72** 715-732.

[10] Ren K, Abdoulaev G S, Bal G and Hielscher A H 2004 Algorithm for solving the equation of radiative transfer in the frequency domain *Optics Letters* **29**(6) 578-580.

[11] Ren K, Bal G and Hielscher A H 2006 Frequency-domain optical tomography based on the equation of radiative transfer *SIAM Journal of Scientific Computing* **28**(4) 1463-1489.

[12] Boulanger J and Charette A 2005 Numerical developments for short-pulsed near infra-red laser spectroscopy. Part II: inverse treatment *Journal of Quantitative Spectroscopy and Radiative Transfer* **91** 297-318.

[13] Kim H K and Charette A 2007 A sensitivity function-based conjugate gradient method for optical tomography with the frequency-domain equation of radiative transfer *Journal of Quantitative Spectroscopy and Radiative Transfer* **104**(1) 24-39.

[14] Kim H K and Charette A 2007 Frequency domain optical tomography using a conjugate gradient method without line search *Journal of Quantitative Spectroscopy and Radiative Transfer* **10**4(2) 248-256.

[15] Boulanger J and Charette A 2005 Reconstruction optical spectroscopy using transient radiative transfer equation and pulsed laser: a numerical study *Journal of Quantitative Spectroscopy and Radiative Transfer* **93** 325-336.

[16] Guo Z, Kumar S and San K-C 2000 Multidimensional Monte Carlo simulation of short-pulse transport in scattering media *Journal of Thermophysics and Heat Transfer* **14**(4) 504-511.

[17] Sawetprawichkul A, Hsu P-F, Mitra K and Sakami M 2000 A Monte Carlo study of transient radiative transfer within the one-dimensional multi-layered slab *Proceedings of the ASME* **366**(1) 145-153.

[18] Lu X and Hsu P-F 2005 Reverse Monte Carlo simulations of light pulse propagation in nonhomogeneous media *Journal of Quantitative Spectroscopy and Radiative Transfer* **93** 349-367.

[19] Kumar S and Mitra K 1998 Microscale aspects of thermal radiation transport and laser applications. *Advances in Heat Transfer* **33** 187-294.

[20] Wu C-Y and Ou N-R. 2002 Differential approximations for transient radiative transfer through a participating medium exposed to collimated irradiation *Journal of Quantitative Spectroscopy and Radiative Transfer* **73** 111-120.

[21] Guo Z and Kumar S 2001 Radiation element method for transient hyperbolic radiative transfer in plane-parallel inhomogeneous media *Numerical Heat Transfer part B* **39** 371-387.

[22] Sakami M, Mitra K and Hsu P-F 2000 Transient radiative transfer in anisotropically scattering media using monotonicity-preserving schemes *Proceedings of the ASME* **366**(1) 135-143.

[23] Sakami S, Mitra K and Hsu P-F 2002 Analysis of light transport through two-dimensional scattering and absorbing media *Journal of Quantitative Spectroscopy and Radiative Transfer* **73** 169-179.
[24] Boulanger J and Charette A 2005 Numerical developments for short-pulsed near infra-red laser spectroscopy. Part I: direct treatment *Journal of Quantitative Spectroscopy and Radiative Transfer* **91** 189-209.
[25] Wu S-H and Wu C-Y 2000 Integral equation solution for transient radiative transfer in nonhomogeneous anisotropically scattering media *ASME Journal of Heat Transfer* **122** 818-822.
[26] Tan Z-M and Hsu P-F 2001 An integral formulation of transient radiative transfer *ASME Journal of Heat Transfer* **123** 466-475.
[27] Katika K M and Pilon L 2004 Backward method of characteristics in radiative heat transfer *Proceedings of the 4th International Symposium on Radiative Transfer (Istanbul, Turkey, 20-25 June 2004)* 347-356.
[28] Katika K M and Pilon L 2004 Ultra-short pulsed laser transport in a multilayered turbid media *Proceedings of IMECE (Anaheim, USA, 13-19 November 2004)* IMECE2004-59796.
[29] Rath P, Mishra S C, Mahanta P, Saha U K and Mitra K 2003 Discrete transfer method applied to transient radiative transfer problems in participating medium *Numerical Heat Transfer A* **44** 183-197.
[30] Okutucu T, Yener Y and Busnaina A A 2007 Transient radiative transfer in participating media with pulse-laser irradiation – an approximate Galerkin solution *Journal of Quantitative Spectroscopy and Radiative Transfer* **103**(1) 118-130.
[31] Okutucu T and Yener Y 2006 Radiative transfer in participating media with collimated short-pulse Gaussian irradiation *Journal of Physics D: Applied Physics* **39** 1976-1983.
[32] Francoeur M, Rousse D R and Vaillon R 2003 Analyse du transfert radiatif instationnaire en milieu semi-transparent absorbant et diffusant *Proceedings of VI^{e} Colloque Interuniversitaire Franco-Québécois (Quebec, Canada, 26-28 May 2003)* 08-07.
[33] Stone J M and Mihalas D 1993 Upwind monotonic interpolation methods for the solution of the time dependent radiative transfer equation *Journal of Computational Physics* **100**(2) 402-408.
[34] Ayranci I and Selçuk N 2004 MOL solution of DOM for transient radiative transfer in 3-D scattering media *Journal of Quantitative Spectroscopy and Radiative Transfer* **84** 409-422.
[35] Elaloufi R, Carminati R and Greffet J J 2002 Time-dependent transport through scattering media: from radiative transfer to diffusion *Journal of Optics A: Pure and Applied Optics* **4**(5) S103-S108.
[36] Francoeur M, Vaillon R and Rousse D R 2005 Theoretical analysis of frequency and time-domain methods for optical characterization of absorbing and scattering media *Journal of Quantitative Spectroscopy and Radiative Transfer* **93** 139-150.
[37] Liu L H and Hsu P-F 2007 Analysis of transient radiative transfer in semitransparent graded index medium *Journal of Quantitative Spectroscopy and Radiative Transfer* **105**(3) 357-376.
[38] Hielscher A H, Liu H, Chance B, Tittel F K and Jacques S L 1996 Time-resolved photon emission from layered turbid media *Applied Optics* **35** (4) 719-728.
[39] Modest M F 2003 *Radiative Heat Transfer* 2nd edition (Academic Press, San Diego).
[40] Rousse D R 2000 Numerical predictions of two-dimensional conduction, convection, and radiation heat transfer. I – formulation *International Journal of Thermal Sciences* **39**(3) 315-331.
[41] Leveque R J 2002 *Finite Volume Methods for Hyperbolic Problems* (University Press, Cambridge).
[42] Colella P and Woodward P R 1984 The piecewise parabolic method (PPM) for gas-dynamical simulations *Journal of Computational Physics* **54** 174-204.